International Journal of Agricultural Technology 2024 Vol. 20(2):877-892
Available online http://www.ijat-aatsea.com
ISSN 2630-0192 (Online)

Effects of NaOH/urea solution as a solvent and salt crystals as a porogen on the fabrication of porous composite scaffold of bacterial cellulose-chitosan for tissue engineering

Yodsanga, S.[1*] and Poeaim, S.[2*]

[1]Department of Oral Pathology, Faculty of Dentistry, Chulalongkorn University, Bangkok 10330, Thailand; [2]Department of Biology, School of Science, King Mongkut's Institute of Technology Ladkrabang (KMITL), Ladkrabang, Bangkok 10520, Thailand.

Yodsanga, S. and Poeaim, S. (2024). Effects of NaOH/urea solution as a solvent and salt crystals as a porogen on the fabrication of porous composite scaffold of bacterial cellulose-chitosan for tissue engineering. International Journal of Agricultural Technology 20(2):877-892.

Abstract A bacterial cellulose-chitosan composite scaffold fabricated through solvent casting-particular leaching method using NaOH/urea solution as a solvent and salt crystals as a porogen revealed a three-dimensional structure with the high porosity investigated by scanning electron microscope. The average porous size of the composite scaffold was between 300 and 500 um. The composite scaffold exhibited high water uptake, indicating to enhance water absorption capacity. The compressive test showed that the composite scaffold had good mechanical strength. Fourier-transform infrared spectroscopy analysis confirmed that bacterial cellulose and chitosan were found to be the main components of the composite scaffold. These results indicated that bacterial cellulose-chitosan composite scaffold could be used for application in tissue engineering.

Keywords: Bacterial cellulose, Chitosan, Composite scaffold, Tissue engineering

Introduction

Cellulose is the most abundant biological polymer on Earth, constituting the primary building block of plant cell walls. The fundamental composition of cellulose consists of recurring glucose molecules connected through β-1,4 glycosidic bonds, forming glucan chains. Intra- and inter-hydrogen bonds between adjacent glucose molecules bind the nascent glucan chains together. Cellulose occurs in plants and can also be synthesized by acetic acid bacteria. Bacterial cellulose (BC) is a colorless, gelatinous substance derived through the fermentation of *Acetobacter xylinum* in a culture medium composed of coconut water or fruit juices. (Lin *et al*., 2013a; Esa *et al*., 2014). It is purer than cellulose from plants due to the absence of other main common polymers, including hemicellulose, pectin and lignin, in its structure (Petersen and Gatenholm, 2011).

[*]**Corresponding Author:** Yodsanga, S.**; Email:** somchai.yo@chula.ac.th, supattra.poe@kmitl.ac.th

BC is generally used as a foodstuff and one ingredient because of its high cellulose content, less energy, and low fat content. Therefore, it is suitable for digestion and controlling weight (Fan *et al*., 2011; Suharno and Nugraha, 2016). Moreover, BC also presents remarkable characteristics, including a three-dimensional (3-D) fibrous network structure with high porosity, high water-holding capacity, mechanical strength, non-toxicity and biocompatibility. The unique qualities of bacterial cellulose (BC) have garnered significant interest as a promising material for scaffolds in tissue engineering applications. (Torgbo and Sukyai, 2018).

A scaffold is a three-dimensional porous network structure material that plays a vital role in tissue-engineering strategies, particularly in the regeneration of bone tissue. The primary goal of a tissue-engineered scaffold is to facilitate cell attachment, proliferation, and differentiation (Baek *et al*., 2022). In addition, it has also been suggested that the scaffolds possess a high porosity (>80%) for bone tissue regeneration. The porous size should be more than 300 um to facilitate the diffusion of nutrients, waste products, cell migration, and new bone tissue formation (Krok-Borkowicz *et al*., 2020; Li *et al*., 2022). BC supports osteoblastic or bone-forming cells' excellent attachment and proliferation. It has also been demonstrated that it does not induce an inflammatory response and maintains sufficient space for bone formation. (Tazi *et al*., 2012; Lee *et al*., 2015; Zhang *et al*., 2020). Moreover, the combination of BC with chitosan has also been fabricated as a composite scaffold to improve cell adhesive and proliferative response (Kim *et al*., 2011; Jia *et al*., 2014).

Following cellulose, Chitosan (CS) stands as the second most abundant natural polysaccharide polymer. It is derived from deacetylated chitin, the primary constituent in the exoskeletons of crustaceans like shells, shrimps, and crabs. CS finds extensive use in diverse biomedical applications owing to its non-toxic, biocompatible, biodegradable, and antimicrobial properties (Oryan and Sahvieh, 2017). Its chemical structure is identical to cellulose, except chitosan has an amino group (NH_2) on C-2 of glucose molecules, whereas the presence of hydroxyl group (OH) on C-2 in cellulose. CS also has a structure similar to glycosaminoglycan, the major component in bone and cartilage extracellular matrix (Ahmed *et al*., 2018). CS has been acknowledged as a promising material in bone tissue engineering, as it can enhance the adhesion and growth of osteoblastic cells. (Zhou *et al*., 2017).

The BC-CS composite materials have been shown to have good mechanical strength antimicrobial activity, improving the proliferation of different cell types and wound healing, which makes them an excellent candidate for wound dressing and scaffolds (Cacicedo *et al*., 2020; Li *et al*., 2017). These composites are fabricated mainly by immersing BC in CS solution. The BC-CS

composites have also been performed with the initial addition of CS into the culture medium (Arikibe *et al*., 2021). They revealed the structural characteristics by scanning an electron microscope and found that CS coats the microfibril network and fills the empty spaces of BC (Cai *et al*., 2009). Although BC has a porous 3-D network structure with pores of various shapes and sizes that are scaffold requirements, it contains porous sizes of 20-60 nm in diameter, which are pretty small (Kheiry *et al*., 2018). In contrast, the infiltration of CS causes the formation of a denser network structure and further reduces BC's porous sizes. This is the main drawback of using BC-CS composites as a bone-engineered scaffold (Phisalaphong and Jatupaiboon, 2008).

The solvent casting-particulate leaching (SCPL) method is the most prevalent technique for crafting porous scaffolds in tissue engineering. It is widely used owing to the simple operation, and the porosity and the porous size of scaffolds are well created through the particle size and the amount of the incorporated porogen particles. This method involves incorporating porogen particles into a casting biopolymer dissolved in the solvent, followed by solvent and porogen removal, leaving behind a porous scaffold (Huang *et al*., 2014). This method considers sodium chloride or salt crystals suitable porogen particles. It can be applied in many soluble biopolymers to create large pores with high porosity in scaffolds and can be quickly and completely removed by washing in distilled water (Aboudzadeh *et al*., 2021).

Sodium hydroxide (NaOH)/urea aqueous solution is well-known as a solvent for cellulose and has been successfully applied to dissolve BC (Pandey *et al*.,2014). CS can also be dissolved in this solvent, possibly because it has a similar chemical structure to BC (Lu *et al*., 2022). The NaOH/urea aqueous solution has been considered simple, harmless, and cheap. BC and CS readily dissolve in a sodium hydroxide (NaOH)/urea aqueous solution (7:12:81 by weight) under low temperatures (-12 °C). The result of the dissolution has shown that BC and CS can transform into a solid gel at room temperature and exhibit good biocompatibility, non-toxicity and mechanical strength (Li *et al*., 2014; Wang *et al*., 2020).

Therefore, the objective was to modify the pore structure and sizes within the BC-SC composite scaffold for tissue engineering applications using the solvent casting-particulate leaching (SCPL) method. This method employed a NaOH/urea aqueous solution as a solvent and salt crystals as porogens.

Materials and methods

The BC powder, generated through the fermentation of *Acetobacter xylinum* TISTR 975 in a coconut water medium, was generously provided by the Biomaterial Testing Center, Faculty of Dentistry, Chulalongkorn University,

Thailand. An aqueous solution of NaOH/urea was utilized as a solvent for dissolving both BC and CS. The solution was prepared by combining NaOH, urea, and distilled water in proportions of 7:12:81 by weight. The mixture was stirred for 10 minutes to achieve a uniform aqueous solution. Once the suspension transformed into a clear solution, the NaOH/urea aqueous solution was retained and pre-cooled at -12 °C before being utilized.

Preparation of BC-CS composite scaffold

The procedural steps for fabricating the BC-CS composite scaffold are illustrated in Figure 1. In summary, 1g of CS, sourced from shrimp shells with a deacetylation degree of ≥75% (Sigma-Aldrich, St. Louis, MO, USA), was dissolved in 100 ml of a pre-cooled NaOH/urea aqueous solution at -12 °C. The mixture was stirred for 30 minutes at room temperature. The blend was placed in a refrigerator at -20 °C overnight, followed by thawing and gentle stirring at room temperature. This freeze-thaw treatment process was iterated six times to achieve transparent CS solution. After that, 1g of BC powder was mixed in CS solution and then placed under -12 °C until it turned into a homogenous and transparent solution. Next, 80g of sieve NaCl or salt crystals with a diameter ranging from 450 to 500 um was added and dispersed in the mixture by a glass rod. The mixture was cast in glass tubes (size 2.5x6 cm) and placed at room temperature overnight to transform into solid gels. BC-CS composite without incorporating salt crystals was also cast and prepared for comparison with the mixture with salt crystals. After complete solidification, all the solid gels were immersed in distilled water several times at room temperature until the pH of the distilled water was 7. This step was provided for salt leaching and solvent removal. Finally, the solid gels were placed in a refrigerator at -20 °C overnight and then freeze-dried under vacuum pressure at -50 °C for 24 hours before further examinations.

Characterization of BC-CS composite scaffolds

Scanning electron microscope (SEM)

The scanning electron microscope (FEI Quanta 250, Netherlands) was employed to investigate the porous structure and dimensions of the BC-CS composite scaffolds. The BC-CS composite scaffolds underwent precise horizontal sectioning using a surgical blade. Subsequently, these sections were affixed to an aluminum stub using two strips of adhesive tape and subjected to gold sputtering before imaging. The gold-coated scaffolds were visually examined and photographed using SEM at an accelerating voltage ranging from

15 to 20 kV. Subsequently, the porous sizes of the BC-CS composite scaffolds were quantified from the SEM images using Image J software.

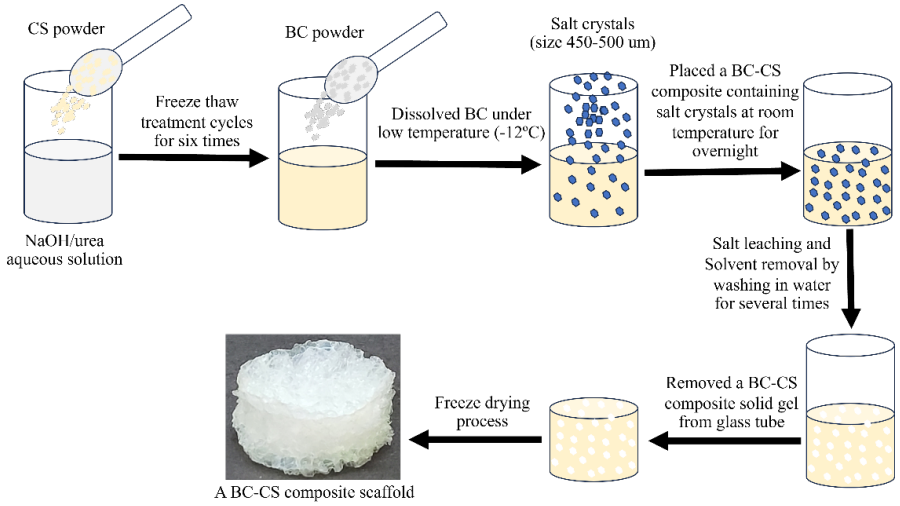

Figure 1. Schematic representation of the BC-CS composite scaffold preparation through the solvent casting-particulate leaching (SCPL) method. NaOH/urea aqueous solution is the solvent, and salt crystals function as porogen particles

Porosity measurement

The total porosity of the BC-CS composite scaffolds was determined through the liquid displacement method. The BC-CS composite scaffolds were initially submerged in a glass tube containing a specified volume of ethanol (V1) for 48 hours. The combined volume of ethanol and BC-CS composite scaffold (V2) was measured after immersion. The residual volume of ethanol (V3) was recorded after removing the BC-CS composite scaffold from ethanol. The porosity percentage (P) of the composite scaffold was subsequently calculated using the following equation:

$$P\ (\%) = \frac{(V1-V3)}{(V2-V3)} \times 100$$

Three replicates were employed for each composite scaffold, and the average porosity value across the various scaffolds was determined.

Fourier transform infrared (FTIR) spectroscopy

The chemical structure of BC-CS composite scaffolds was examined through Fourier transform infrared (FTIR) spectroscopy using equipment from Perkin Elmer Scientific, Waltham, USA. The composite scaffolds were ground and mixed with potassium bromide to prepare the samples. During FTIR

analysis, the spectra of BC-CS composite scaffolds were captured at a resolution of 4 cm^{-1} within a wavelength range of 4000 to 400 cm^{-1}.

Water absorption capacity

The water absorption capacity of BC-CS composite scaffolds was assessed by immersing them in distilled water at room temperature until reaching equilibrium. Before the examination, the weight of each scaffold was recorded. Following immersion, the composite scaffolds were delicately taken out of distilled water, positioned on a filter paper to allow excess water to drain, and promptly weighed. The percentage of water absorption was calculated using the following equation:

$$\text{Water absorption (\%)} = \frac{W_f - W_i}{W_i} \times 100$$

Where Wi represents the initial weight of the scaffolds, and Wf is the weight of the scaffolds after immersion. This examination was performed on three separate scaffolds, and the mean value was calculated to ensure reliable data.

Compressive test

The mechanical strength of BC-CS composite scaffolds was assessed through compressive tests conducted in dry and wet states using the universal testing machine (INSTRON model 8872, England) at the Dental Materials R&D Center, Faculty of Dentistry, Chulalongkorn University. The testing procedure followed the guidelines outlined in ASTM D5024-95a. The mechanical property test utilized BC-CS composite scaffolds with a diameter of 5x10 mm. A 250 N load cell was employed at a 0.5 mm min^{-1} rate until the composite scaffold was compressed to 50% of its original thickness. The compression values were recorded and calculated using three replicates for each BC-CS composite scaffold.

Results

The dissolution state of BC and CS in NaOH/urea aqueous solution could be observed via an optical microscope and the naked eye. As shown in Figure 2, CS could be wholly dissolved in an aqueous NaOH/urea solution via a freeze-thawing method. In addition, it can be seen that the combination of BC and CS completely dissolved in NaOH/urea aqueous solution under low temperature, which displayed a transparent solution (Figure 3A-B). After overnight incubation at room temperature, the BC-CS composite incorporated and without salt crystals turned from a transparent solution to white solid gels that were insoluble in water (Figure 3C-D).

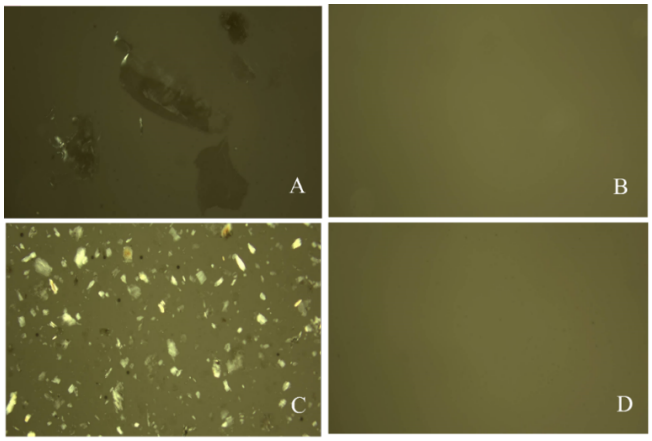

Figure 2. Microscopic images were captured using a 4X objective lens, depicting various stages in the process: (A) chitosan in NaOH/urea aqueous solution, (B) Chitosan dissolved in NaOH/urea aqueous solution after five cycles of freeze-thaw treatments, (C) Bacterial cellulose (BC) in chitosan (CS) solution containing NaOH/urea and (D) BC dissolved in CS solution containing NaOH/urea under low temperature

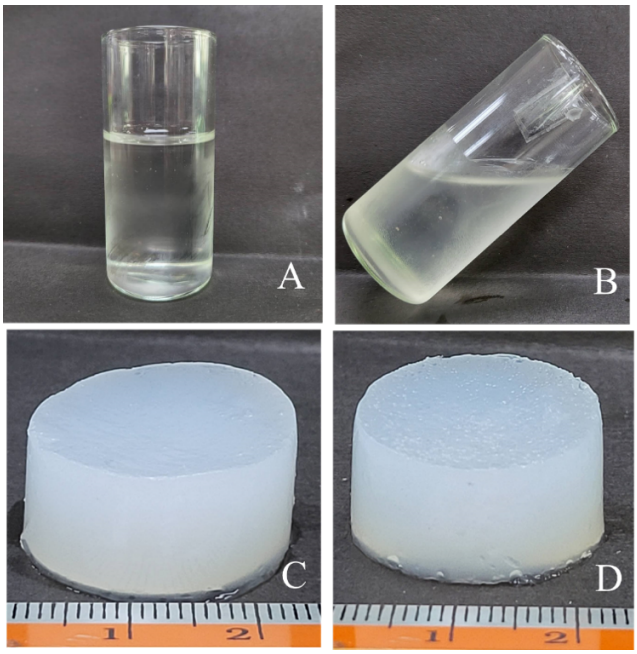

Figure 3. Here are descriptions for the images: (A) transparent chitosan (CS) solution, (B) bacterial cellulose-chitosan (BC-CS) solution when tilted, (C) BC-CS solid gel without salt crystals and (D) BC-CS solid gel with mixed salt crystals

The structural characteristics of BC-CS composite scaffolds were revealed after the freeze-dried process using SEM. The SEM micrographs of BC-CS composite scaffolds exhibited a homogenous porous structure and porous sizes (Figure 4). The leaching out of salt crystals from the BC-CS composite scaffold left the porous structure with evenly distributed pores behind. The irregular porous sizes were obtained with average pore dimensions ranging from 325-497 um. While the BC-CS composite scaffold fabricated without incorporating salt crystals in the SCPL method presented the pores throughout the structural scaffold, it showed very different porous sizes ranging from between 10 and >500 um with a more compact structure.

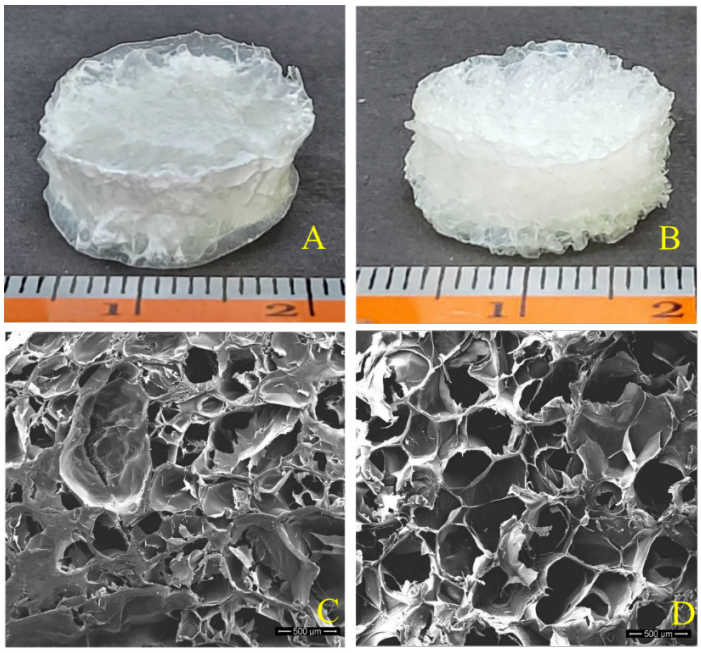

Figure 4. Photographs and scanning electron microscope (SEM) images were taken at 100X magnification to capture the freeze-dried BC-CS composite scaffold in two conditions: without salt crystal incorporation (A and C) and with the inclusion of salt crystals using the SCPL method (B and D)

The porosity measurement results obtained through the liquid displacement method revealed the high porosity of BC-CS composite scaffolds, as shown in Table 1. The BC-CS composite scaffold demonstrated a porosity percentage of 92 ± 2.66%. In contrast, the porosity percentage of the BC-CS composite scaffold, fabricated without incorporating salt crystals in the SCPL method, was 70 ± 2.08%. The elevated porosity observed in the BC-CS composite scaffold

was attributed to the presence of salt crystals. This finding aligns with the SEM observations, corroborating the uniform porosity evident in the BC-CS composite scaffold manufactured through the SCPL method.

Table 1. Comparative analysis of porosity, water absorption capacity and compressive strength of BC-CS composite scaffolds (Mean±standard deviation)

Scaffold type	Porosity (%)	Water absorption capacity (%)	Compressive strength (MPa)	
			Dry state	Wet state
BC-CS	92±2.66%	60.8±1.4%	1.3±0.12	0.62±0.07
BC-CS (without the incorporation of salt crystals in the SCPL method)	70±2.08%	68.8±1.6%	2.05±0.40	0.84±0.09

The FTIR spectra of BC-CS composite scaffolds presented the wave numbers 1000 to 4000 (Figure 5). The peak characteristics of BC were at 3000 to 3500 cm^{-1} due to the presence of stretching vibrations for O-H. The peak characteristics of CS were observed in the absorption bands at 1645, 1436 and 1276 cm^{-1} . The identified bands corresponding to amide-I, amide-II, and amide-III groups indicate the presence of chitosan (CS) molecules. The peak observed at 1042 cm-1 is also attributed to the C-O-C pyranose ring skeletal stretching vibration. The FTIR spectra results are crucial in confirming the existence of both BC and CS molecules within these composite scaffolds.

The water absorption capacity was defined by weighing the before and after placing BC-CS composite scaffolds in distilled water. As shown in Table 1, the results showed that the BC-CS composite scaffold absorbed distilled water up to 60.8% of its dry weight. Meanwhile, the BC-CS composite scaffold fabricated without the incorporation of salt crystals in the SCPL method was 68.8% of its dry weight. Therefore, these results indicated that BC-CS composite scaffolds had a high water absorption capacity. Compressive property of BC-CS composite scaffolds was examined in both the dry and wet states. Compressive test results on BC-CS composite scaffolds in the dry and wet states were 1.3±0.12 and 0.62±0.07 MPa on average. In contrast, the results of compressive test BC-CS composite scaffolds fabricated without incorporating salt crystals in the SCPL method were 2.03±0.40 MPa in the dry state and 0.85±0.09 MPa in the wet state. These results detemined that compressive properties of BC-CS composite scaffolds in the wet state decreased compared to the dry state.

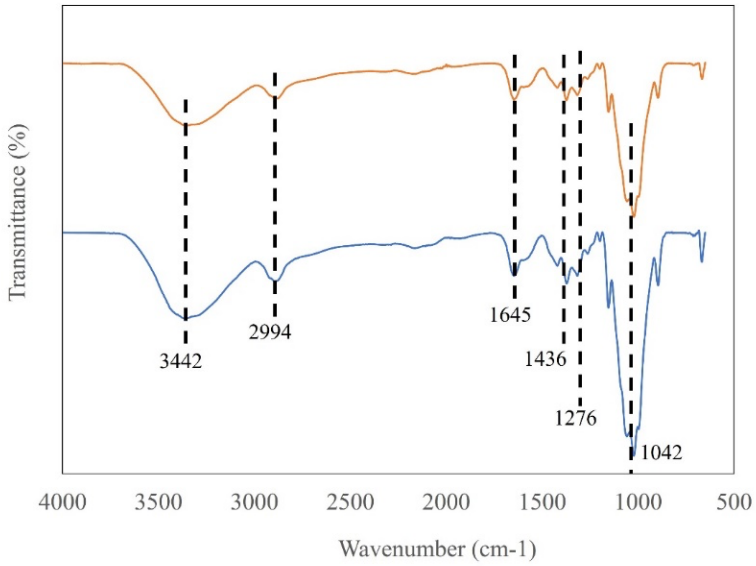

Figure 5. FTIR spectra of BC-CS composite scaffolds without (orange line) and the incorporation of the salt crystals (blue line) in SCPL method

Discussion

In this work, NaOH/urea aqueous solution and salt crystals were essential in fabricating BC-CS composite scaffolds through an SCPL method. CS and BC could be wholly dissolved in an aqueous NaOH/urea solution by freeze-thaw treatments and under low temperatures. After freeze-thaw treatments at five cycles, a transparent solution of CS was obtained. This is in line with the research of Zhang and Xia (2014), who suggested that the dissolution of CS increased with the increasing cycles of freeze-thaw treatments. When BC was added and dispersed in a CS solution containing NaOH/urea at -12 °C, it could also be completely dissolved within a few minutes. Mao et al. (2020) documented that BC readily dissolved in an aqueous NaOH/urea/water system at a weight ratio of 7:12:81 under low temperatures ranging from -12 °C. This process resulted in the formation of a transparent BC solution. In this solvent system, NaOH was found that can penetrate to BC and CS molecules under low temperatures to destroy the intra- and inter-hydrogen bonds, while urea prevented the interaction between the chemical molecules BC and CS through hydrogen bonds (Phisalaphong *et al*., 2008; Hu *et al*., 2007).

Salt crystals successfully improved the porosity and porous sizes of the BC-CS composite scaffold. The results of this work revealed that the BC-CS composite scaffold possessed a high porosity (>90%) with a large porous size of

300-500 um, evenly distributed throughout the structural scaffold. Coogan *et al*. (2020) and Xie *et al*. (2021) reported that salt crystals can create and improve porosity and large pores in scaffold fabrication through a SCPL method. The BC-CS composite scaffold fabricated without incorporating salt crystals in the SCPL method exhibited different small and large pore distributions in the structural scaffold affected by freeze-drying. This method not only served for drying the scaffolds but also played a crucial role in generating pores within the structural framework. Nevertheless, it is worth noting that controlling the porosity and the sizes of created pores during the freeze-drying process posed significant challenges, as Shahbazarab *et al*. (2018) pointed out.

Due to the close similarity in the chemical structures of BC and CS molecules, it was anticipated that these two biopolymers could be effectively combined while retaining their inherent biocompatibility properties. The FTIR analysis was provided to detect the chemical molecules of the BC-CS composite. Savitskaya *et al*. (2017) reported that the peak characteristics of BC were 3000-3500 cm^{-1} due to O-H stretching. In addition, Lin *et al*. (2013b) and Jia *et al*. (2017) reported that some additional peaks also appeared in the spectra of the combination of BC and CS corresponding to the peak characteristics of amide I, II and III bands of CS. For the BC-CS composite scaffold, the results of the FTIR analysis showed the presence of almost all the peak characteristics of BC and CS. This indicated that the chemical component of BC and CS was not charged after the fabrication, and the solvent and salt crystals had been completely removed (Wahid *et al*., 2019). The investigation of the water absorption capacity showed that the BC-CS composite scaffold absorbed water up to 60 times its dry weight.

On the other hand, Ul *et al*. (2011) and Magpoc *et al*. (2018) reported that the water absorption capacity of BC-CS composite membranes was 97 and 87 times their dry weight, respectively. These composite membranes were fabricated by immersing BC in CS solution. The result indicated that BC-CS composite membranes had a high- water absorption capacity, affecting the fibrous network structure of natural BC.

To evaluate the mechanical strength, this evaluation showed that the compressive modulus of BC-CS composite scaffolds in the dry state was higher than that in the wet state. Moreover, BC-CS composite scaffolds in dry and wet states were not brittle or broken during the compressive test. This indicated that BC-CS composite scaffolds were strong enough to maintain structural unity. In particular, the studies of wet state were executed as close to in vitro and in vivo conditions as possible to ensure the scaffold's suitability for bone tissue engineering application. However, the porosity and porous sizes of fabricated scaffolds also affect their mechanical strength (Li *et al*., 2018). The compressive

modulus of BC-CS composite scaffold in dry and wet states fabricated without the incorporation of salt crystals in the SCPL method was higher than (2.03 MPa and 0.85 MPa) BC-CS composite scaffold fabricated by incorporating salt crystals in the SCPL method compressive modulus (1.3 and 0.62 MPa). This study found that the high porosity and greatest porous sizes of BC-CS composite scaffold resulted in decreased mechanical strength. This is in line with the research of Thadavirul *et al*. (2014) and Mallick *et al*. (2018), who reported that the decreased compressive properties of the scaffolds are related to the highly porous structure with the greatest pores. Besides, Zaborowska *et al*. (2010) also reported that the compressive strength of the fabricated scaffolds was lower than or close to the lower limit of compressive strength in human cancellous bone (2-10 MPa). This scaffold might be proper for bone healing in non-bearing sites such as the face and skull bones.

Hence, the findings indicate that the BC-CS composite scaffold, crafted through the SCPL method utilizing NaOH/urea aqueous solution as a solvent and incorporating salt crystals as a porogen, holds promise as a prospective candidate for future bone tissue engineering applications.

Acknowledgments

We thank the Biomaterial Testing Center and Department of Oral Pathology, Faculty of Dentistry, Chulalongkorn University, Bangkok 10330, Thailand, for bacterial cellulose powder and laboratory instruments.

References

Aboudzadeh, N., Khavandi, A., Javadpour, J., Shokrgozar, M. A. and Imani, M. (2021). Effect of dioxane and N-methyl-2-pyrrolidone as a solvent on biocompatibility and degradation performance of PLGA/nHA Scaffolds. Iranian Biomedical Journal, 25:408-416.

Ahmed, S., Ali, A. A. and Sheikh, J. (2018). A review on chitosan centred scaffolds and their applications in tissue engineering. International Journal of Biological Macromolecules, 116:849-862.

Arikibe, J. E., Lata, R. and Rohindra, D. (2021). Bacterial cellulose/chitosan hydrogels synthesized in situ for biomedical application. Journal of Applied Biosciences, 162:16675-16693.

Baek, J. W., Kim, K.S., Park, H. and Kim, B. S. (2022). Marine plankton exoskeleton derived hydroxyapatite/polycaprolactone composite 3D scaffold bone for bone tissue engineering. Biomaterials Science, 224:7055-7066.

Cacicedo, M. L., Pacheco, G., Islan, G. A., Alvarez, V. A., Barud, H. S. and Castro, G. R. (2020). Chitosan-bacterial cellulose patch of ciprofloxacin for wound dressing: Preparation and

characterization studies. International Journal of Biological Macromolecules, 147:1136-1145.

Cai, Z., Chen, P., Jin, H. J. and Kim, J. (2009). The effect of chitosan content on the crystallinity, thermal stability, and mechanical properties of bacterial cellulose-chitosan composites. Journal of Mechanical Engineering Science, 223:2225-2230.

Coogan, K. R., Stone, P. T., Sempertegui, N. D. and Rao, S. S. (2020). Fabrication of micro-porous hyaluronic acid hydrogels through salt leaching. European Polymer Journal, 135:109870.

Esa, F. Tasirin, S.M. and Rahman, N. A. (2014). Overview of bacterial cellulose production and application, Agriculture and Agricultural Science Procedia, 2:113-119.

Fan, H., Wu, Y., Hu, X., Wu, J. and Liao, X. (2011). Characteristics of thin-layer drying and rehydration of nata de coco. Food Science and Technology, 46:1438-1444.

Hu, X., Du, Y., Tang, Y., Wang, Q., Feng, T., Yang, J. and Kennedy, J. F. (2007). Solubility and property of chitin in NaOH/urea aqueous solution. Carbohydrate Polymers, 70:451-458.

Huang, R., Zhu, X., Zhao, T. and Wan, A. (2014). Preparation of tissue engineering porous scaffold with poly(lactic acid) and polyethylene glycol solution blend by solvent-casting/particulate-leaching. Materials Research Express, 1:045403.

Jia, Y., Wang, X., Huo, M., Zhai, X., Li, F. and Zhong, C. (2017). Preparation and characterization of a novel bacterial cellulose/chitosan bio-hydrogel. Nanomaterials and Nanotechnology, 7:1-8.

Jia, Y., Wei, Z., Fu, W., Huo, M., Li, F., Zhong, C., Jia, S. and Zhou, Y. (2014). Biocompatibility evaluation on a bio-hydrogel composed of bacterial cellulose and chitosan. Journal of Biomaterials and Tissue Engineering, 4:118-112.

Kheiry, E. V., Parivar, K., Baharara, J., Fazly Bazzaz, B. S. and Iranbakhsh, A. (2018). The osteogenesis of bacterial cellulose scaffold loaded with fisetin. Iran Journal of Basic Medical Sciences, 21:965-971.

Kim, J., Cai, Z., Lee, H. S., Choi, G. S., Lee, D. H. and Jo, C. (2011). Preparation and characterization of a bacterial cellulose/chitosan composite for potential biomedical application. Journal of Polymer Research, 18:739-744.

Krok-Borkowicz, M., Reczynska, K. L., Menaszek, E., Orzelski, M., Malisz, P., Silmanowicz, P., Dobrzynski, P. and Pamula, E. (2020). Surface-modified poly(l-lactide-*co*-glycolide) scaffolds for the treatment of osteochondral critical size defects-in vivo studies on rabbits. International Journal of Molecular Sciences, 21:7541.

Lee, S. H., Lim, Y. M., Jeong, S. I., An, S. J., Kang, S. S., Jeong, C. M. and Huh, J. B. (2015). The effect of bacterial cellulose membrane compared with collagen membrane on guided bone regeneration. Journal of Advance Prosthodontists, 7:484-495.

Li, C., Han, Q., Guan, Y. and Zhang, Y. (2014).Thermal gelation of chitosan in an aqueous alkali-urea solution. Soft Matter, 10:8245-8253.

Li, G., Nandgaonkar, A. G., Habibi, Y., Krause, W. E., Wei, Q. and Lucia, L. A. (2017). An environmentally benign approach to achieving vectorial alignment and high microporosity in bacterial cellulose/chitosan scaffolds. RSC Advances, 7:13678-13688.

Li, J., Wang, C., Gao, G., Yin, X., Pu, X., Shi, B., Liu, Y., Huang, Z., Wang, J., Li, J. and Yinn, G. (2022). MBG/ PGA-PCL composite scaffolds provide highly tunable degradation and osteogenic features, Bioactive Materials, 15:53-67.

Li, Y., Zhang, Z. and Zhang, Z. (2018). Porous chitosan/nano-hydroxyapatite composite scaffolds incorporating simvastatin-loaded PLGA microspheres for bone repair. Cells Tissues Organs, 205:20-31.

Lin, S. P., Loira, C. I., Catchmark, J. M., Liu, J. R., Demirci, A. and Cheng, K. C. (2013a). Biosynthesis, production and applications of bacterial cellulose. Cellulose, 20:2191-2219.

Lin, W. C., Lien, C. C., Yeh, H. J., Yu, C. M. and Hsu, S. H. (2013b). Bacterial cellulose and bacterial cellulose-chitosan membranes for wound dressing applications. Carbohydrate Polymers, 94:603-611.

Lu, Z., Zou, L., Zhou, X., Huang, D. and Zhang, Y. (2022). High strength chitosan hydrogels prepared from NaOH/urea aqueous solutions: the role of thermal gelling. Carbohydrate Polymers, 297:120054.

Magpoc, R. L., Garcia, J. E. A., Tayo, L. L. and Sauli, Z. (2018). Preparation and characterization of bacterial cellulose-chitosan composite as antimicrobial material. International Journal of Nanoelectronics and Materials, 11:23-32.

Mallick, S. P., Singh, B. N., Rastogi, A. and Srivastava, P. (2018). Design and evaluation of chitosan/poly(l-lactide)/pectin based composite scaffolds for cartilage tissue regeneration. International Journal of Biological Macromolecules, 112:909-920.

Mao, L., Hu, S., Gao, Y., Wang, L., Zhao, W., Fu, L., Cheng, H., Xia, L., Xie, S., Ye, W., Shi, Z. and Yang, G. (2020). Biodegradable and electroactive regenerated bacterial cellulose/MXene ($Ti_3 C_2 T_x$) composite hydrogel as wound dressing for accelerating skin wound healing under electrical stimulation. Advanced Healthcare Materials, 9:200872.

Oryan, A. and Sahvieh, S. (2017). Effectiveness of chitosan scaffold in skin, bone and cartilage healing. International Journal of Biological Macromolecules, 104:1003-1011.

Pandey, M., Abeer, M. M. and Amin, M. C. I. (2014). Dissolution study of bacterial cellulose (nata de coco) from local food Industry: solubility behavior & structural changes. International Journal of Pharmacy and Pharmaceutical Sciences, 6:89-93.

Petersen, N. and Gatenholm, P. (2011). Bacterial cellulose-based materials and medical devices: current state and perspectives. Applied Microbiology Biotechnology, 91:1277-1286.

Phisalaphong, M. and Jatupaiboon, N. (2008). Biosynthesis and characterization of bacteria cellulose-chitosan film. Carbohydrate Polymers, 74:482-488.

Phisalaphong, M., Suwanmajo, T. and Sangtherapitikul, P. (2008). Novel nanoporous membranes from regenerated bacterial cellulose. Journal of Applied Polymer Science, 107:292-299.

Savitskaya, I. S., Kistaubayeva, A. S., Digel, I. E. and Shokatayeva, D. H. (2017). Physicochemical and antibacterial properties of composite films based on bacterial cellulose and chitosan for wound dressing materials. Euransian Chemico-Technological Journal, 19:255-264.

Shahbazarab, Z., Teimouri, A., Chermahini, A. N. and Azadi, M. (2018). Fabrication and characterization of nanobiocomposite scaffold of zein/chitosan/nanohydroxyapatite prepared by freeze-drying method for bone tissue engineering. International Journal of Biological Macromolecules, 108:1017-1027.

Suharno, S. N. J. and Nugraha, D. A. (2016). Development of nata de coco with natural dyes using value engineering method. The 3rd International Conference on Agro-Industry, 96-109.

Tazi, N., Zhang, Z., Messaddeq, Y., Almeida-Lopes, L., Zanardi, L. M., Levinson, D. and Rouabhia, M. (2012). Hydroxyapatite bioactivated bacterial cellulose promotes osteoblast growth and the formation of bone nodules. AMB Express, 2:61.

Thadavirul, N., Pavasant, P. and Supaphol, P. (2014). Development of polycaprolactone porous scaffolds by combining solvent casting, particulate leaching, and polymer leaching techniques for bone tissue engineering. Journal of Biomedical Materials Research Part A, 102:3379-3392.

Torgbo, S. and Sukyai, P. (2018). Bacterial cellulose-based scaffold materials for bone tissue engineering, Applied Materials Today, 11:34-49.

Ul, I. M., Shah, N., Ha, J.H. and Park, J. K. (2011). Effect of chitosan penetration on physico-chemical and mechanical properties of bacterial cellulose. Korean Journal of Chemical Engineering, 28:1736-1743.

Wahid, F., Hu, X. H., Chu, L. Q., Jia, S. R., Xie, Y. T. and Zhong, C. (2019). Development of bacterial cellulose/chitosan based semi-interpenetrating hydrogels with improved mechanical and antibacterial properties. International Journal of Biological Macromolecules, 122:380-387.

Wang, L., Hu, S., Ullah, M. W., Li, X., Shi, Z. and Yang, G. (2020). Enhanced cell proliferation by electrical stimulation based on electroactive regenerated bacterial cellulose hydrogels. Carbohydrate Polymers, 249:116829.

Xie, Y., Lee, K., Wang, X., Yoshitomi, T., Kawazoe, N., Yang, Y. and Chen, G. (2021). Interconnected collagen porous scaffolds prepared with sacrificial PLGA sponge templates for cartilage tissue engineering. Journal of Materials Chemistry B, 9:8491-8500.

Zaborowska, M., Bodin, A., Backdahl, H., Popp, J., Goldstein, J. and Gatenholm, A. (2010). Microporous bacterial cellulose as a potential scaffold for bone regeneration. Acta Biomaterialia, 6:2540-2547.

Zhang, W. and Xia, W. (2014). Dissolution and stability of chitosan in a sodium hydroxide/urea aqueous solution. Journal of Applied Polymer Science, 131:39819.

Zhang, W., Wang, X. C., Li, X. Y., Zhang, L. L. and Jiang, F. (2020). A 3D porous microsphere with multistage structure and component based on bacterial cellulose and collagen for bone tissue engineering. Carbohydrate Polymers, 236:116043.

Zhou, D., Qi, C., Chen, Y. X., Zhu, Y. J., Sun, T. W., Chen, F. and Zhang, C. Q. (2017). Comparative study of porous hydroxyapatite/chitosan and whitlockite/chitosan scaffolds

for bone regeneration in calvarial defects. International Journal of Nanomedicine, 12:2673-2687.

(Received: 2 November 2023, Revised: 22 January 2024, Accepted: 9 February 2024)